JOURNAL OF AIRCRAFT
Vol. 33, No. 3, May–June 1996

Vortex Model to Define Safe Aircraft Separation Distances

Alexandre Corjon*
STNA, F-75732 Paris, France
and
Thierry Poinsot†
CERFACS, F-31057 Toulouse, France

An approximate model of wake vortices behavior is presented. We have introduced modifications in the Greene's model to take into account the effects of ground (divergence, rebound) and crosswind (advection, shear). Direct numerical simulations of laminar flows with and without lateral wind are performed to validate these extensions. The first results are encouraging and efforts are carried on to derive a more reliable model. The capability of this model to mimic the reality is shown by comparison with an experimental test case.

Nomenclature

A = area of wake oval $2.09\pi/4\sqrt{3}b_0^2$
AR = aspect ratio, b^2/A
b = wingspan
b_0 = initial spacing between primary vortices $\pi/4b$ for an elliptically loaded wing
C_D = drag coefficient, viscous force/$(\rho V^2/2)L$
C_L = lift coefficient, lift force/$[(\rho V^2/2)(S^2/\mathrm{AR})]$
c = chord
g = stream function coefficient of Lamb vortex (used in direct numerical simulation computation)
h = altitude of the vortices
L = width of wake oval $2.09b_0$
N = Brunt–Väisälä frequency
q = rms velocity, $2\Lambda^{1/3}\varepsilon^{1/3} = \sqrt{\overline{u'^2} + \overline{v'^2} + \overline{w'^2}}$, m/s
R_b = core radius after bursting
Re = Reynolds number
Re_Γ = circulation-based Reynolds number, Γ/ν
r_c = core radius
T = temperature
T_b, T_c = bursting, linking time
t = time
V = wake descent speed
x, y, z = ground coordinate
w_0 = crosswind magnitude at initial height
Γ = circulation of individual vortex
γ = ratio of specific heat
ε = turbulent energy dissipation rate
Λ = half of integral length scale of turbulence
ν = kinematic viscosity
ρ = density
σ = wind shear

Subscripts
c = core
0 = initial

Superscripts
* = normalized number
′ = related to secondary vortices

Received May 28, 1995; presented as Paper 95-1776 at the AIAA 13th Applied Aerodynamics Conference, San Diego, CA, June 19–22, 1995; revision received Jan. 26, 1996; accepted for publication Jan. 28, 1996.

*STNA Consultant; currently Senior Researcher, CERFACS, 42 av. G. Coriolis, F-31057 Toulouse, France. Member AIAA.

†CFD Team Manager, Department of Fluid Mechanics. Member AIAA.

Introduction

BEFORE 1970, the quite similar masses of all aircrafts and the low traffic density prevented the hazardous encounter between trailing vortices of an aircraft at landing or takeoff and the following aircraft. With both the Boeing 747 arrival and the constant traffic growth many incidents occur in the terminal area during landing and takeoff.

Between 1969–1976, the Federal Aviation Administration (FAA) has made an extensive data collection effort (flight and ground test and incidents analysis), which led to the definition of aircraft separation standards edited by International Civil Aviation Organization (ICAO) and applied by many countries. The objective of this categorization is to ensure safety by avoiding any encounter. To recover some of the capacity lost, the FAA continued its wake vortex program until 1981. The Vortex Advisory System (VAS) was developed but never operationally agreed on.

The FAA wake vortex program was reactivated in 1984 (ended in 1987), in 1989 (ended in 1991), and finally reactivated again in 1993. The ongoing FAA wake vortex program is performed in cooperation with the NASA Terminal Area Productivity (TAP) program. This multiyear program will furnish several operationally implementable products. The latest (>1998) should be the Aircraft Vortex Spacing System (AVOSS), a comprehensive airport system for providing vortex-based separation constraints to automated air traffic control. The AVOSS will first integrate rules based on validated wake vortex transport characteristics and subsequent knowledge of wake vortex decay and hazard definition.

In Europe, this problem is mainly experienced in England at Heathrow Airport where many incidents caused by wake vortex encounters are reported, and in Frankfort where there are two closely spaced (<2500-ft) parallel runways and no possibility to build a new one.

In France, the most important aircraft delays occur at Orly airport. Acting for the Direction Générale de l'Aviation Civile (DGAC), the Service Technique de la Navigation Aérienne (STNA) has defined objectives to study wake vortices. The first goal is to decrease these delays thanks to an advisory system for air traffic control (ATC) based on short-term wind forecasting. This system will permit reducing momentarily the separations to specified radar minima. In the long term, an automatic system optimizing separations between aircrafts, called SYAGE (Système Anticipatif de Gestion des Espace-

ments) should be integrated in an advanced ATC system, and more realistic categorization criteria should be defined than the maximum take-off weight (MTOW).

It was decided to first develop semiempirical models that allow an estimate of the formation of the trailing vortices, to take into account the effect of meteorological conditions on the vortices behavior and to study the interaction between a vortex and an aircraft.

This article focuses on the vortices behavior model. For the vortex sheet roll-up, a point vortex method[1,2] is used and the initial lift distribution is obtained by the use of a vortex lattice method. To complete the risk model, it is necessary to account for the interaction between an aircraft and a vortex. This interaction model has been developed by ONERA (Ref. 3). It is a five-degree-of-freedom aircraft model based on strip theory.

From an operational point of view, it is necessary to develop such a simple model that can be used in real time. But this model requires a large amount of validation because it comprises many parameters that are difficult to fix. Therefore it was decided to develop not only a simple model, but also complex ones based on a Navier–Stokes solver. These complex models allow cheaper validation of the simple model than experiments. Moreover, many effects considered by these models are not turbulence controlled and may be investigated in laminar flows. Therefore, direct numerical simulations (DNS) of two-dimensional unsteady laminar flows are used. To address turbulence-controlled problems we will use large eddy simulations for three-dimensional unsteady turbulent flows (not presented here).

The next section presents the evolution model that will allow a definition of the safety distance between two aircrafts under given meteorological conditions. The third section describes the validation of this simple code (called VORTEX), using DNS and experimental results.

Vortex Behavior Model

The engineering model assumes first, that the vortex sheet has completely rolled-up, and second, that there are only two counter-rotating vortices. The trajectory computation of more than two primary vortices is possible, but not yet implemented. The initial conditions for a given aircraft can be either the results of the point vortex method or experimental or from another source. Certain external conditions act on vortices to enhance their decay. These external conditions are stratification, atmospheric turbulence, crosswind, wind shear, Crow instability, bursting, and ground effect. The model developed by Greene,[4] which treats the effects of stratification, atmospheric turbulence, and the Reynolds number is modified. The modifications aim at taking also into account the ground and crosswind effects. As these two vortices define a finite rotational core area with a core radius equal to about 10% of the wingspan,[5] which is small in comparison to their spacing b_0, the wake vortices can be represented by two-point vortices. The model determines the trajectories of the two main vortices and their circulation. The effects on circulation decay because of turbulence, stratification, and viscosity are assumed to be linear:

$$\frac{d\Gamma}{dt} = \left.\frac{d\Gamma}{dt}\right|_{\text{viscous}} + \left.\frac{d\Gamma}{dt}\right|_{\text{buoyancy}} + \left.\frac{d\Gamma}{dt}\right|_{\text{turbulence}}$$

If we assume that the vortices are in a still homogeneous inviscid flow, a well-known solution exists. The initial descent speed is $V_0 = \Gamma_0/2\pi b_0$. Inviscid theory shows that there is an associated recirculating mass of fluid included in an oval[6] of axis $(1.73b_0/2, 2.09b_0/2)$. This cell is convected downward at a uniform speed and the outer flow never enters it. In real flows, differing behaviors may be encountered, but these are the basic hypotheses of the Greene's model, except that the descent speed is no longer constant. If the Boussinesq approximation is made, the wake momentum or impulse per unit length may still be defined as $\rho b\Gamma$. Thus, Greene[4] defines the rate of change of the circulation for viscous interaction and buoyancy force as

$$\left.\frac{d\Gamma}{dt}\right|_{\text{viscosity,buoyancy}} = -\frac{F}{\rho b_0} \tag{1}$$

where

$$F|_{\text{viscous}} = -(\rho V^2/2)C_D L$$

$$F|_{\text{buoyancy}} = -\rho A N^2 z$$

The viscous effect is obtained by assuming that the forces acting on the wake are the same as those acting on a similar solid body. For the buoyancy effects, Greene considers that the density inside and outside the wake are the same if the lapse rate in the atmosphere is adiabatic. If not, the two densities will differ and the resulting net buoyancy force could be expressed with N (z define) positive downward-equivalent to $-y$ here).

For atmospheric turbulence, the results of Donaldson and Bilanin[5] are used:

$$\left.\frac{d\Gamma}{dt}\right|_{\text{turbulence}} = -0.82(q\Gamma/b_0) \tag{2}$$

where $q = 2\Lambda^{1/3}\varepsilon^{1/3}$ is related to ε as proposed by Tombach.[7] This model was modified as follows.

Divergence

The first effect of the ground is to make the vortex pair diverge. The assumption made by Greene[4] that there is a constant distance between the two vortices is no longer valid.

This divergence is because of an inviscid phenomenon. The ground plane can be modeled by two image vortices whose strengths are equal and opposite to those of the real vortices to satisfy the slip boundary condition in the inviscid theory.[8] When the real vortex and its image are close enough their mutual interaction has a greater importance than the mutual interaction of the two real vortices.

To take into account the divergence near the ground, Eq. (1) is modified:

$$\left.\frac{d\Gamma}{dt}\right|_{\text{viscosity,buoyancy}} = -(F\cos\theta/\rho b_0) \tag{3}$$

where θ is the angle between the force and the drift velocity of the vortex.

Rebound

Experiments show that the trajectory of the vortices near the ground in the atmosphere does not follow the inviscid trajectory.[9] Harvey and Perry[10] have explained this by conducting an experiment using a half-span wing to generate a single vortex passing over a moving floor in a wind tunnel. During their descent, the vortices induce a very strong vorticity sheet because of the adverse pressure gradient, which becomes unstable and detaches from the wall creating secondary vortices. Liu[11] proposed to modify the classical two-dimensional theory by adding a line vortex near the wall to account for the secondary vortex. The equations for the total induced velocity of the primary vortex become

$$\frac{dx_i}{dt} = \sum_{j\neq i}\frac{\Gamma_j}{2\pi}\frac{y_j - y_i}{r_{ij}^2} + \frac{\Gamma_i'\cos\theta_i}{2\pi r_i'} \tag{4}$$

$$\frac{dy_i}{dt} = \sum_{j\neq i}\frac{\Gamma_j}{2\pi}\frac{x_j - x_i}{r_{ij}^2} + \frac{\Gamma_i'\sin\theta_i}{2\pi r_i'} \tag{5}$$

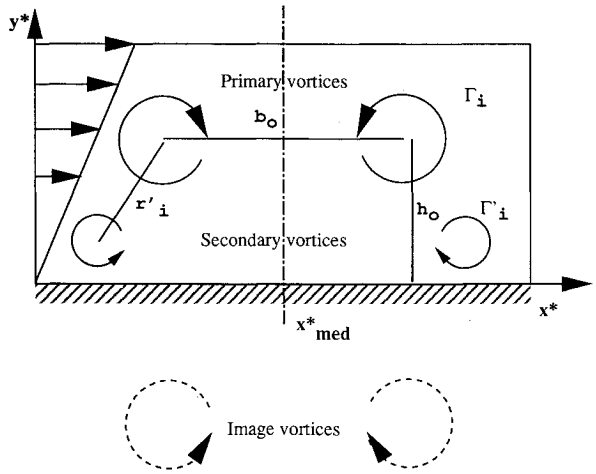

Fig. 1 Computational domain.

$$\frac{d\theta_i}{dt} = \frac{\Gamma_i - \Gamma'_i}{2\pi r_i'^2} \tag{6}$$

$$r_{ij}^2 = (x_j - x_i)^2 + (y_j - y_i)^2 \tag{7}$$

where $i = 1, 2$ and $j = 1, \ldots, 4$.

Γ'_i is the circulation strength of the secondary vortex associated with the primary vortex i, r'_i the constant distance between the secondary and primary vortices, and θ_i the rotation angle of the primary and secondary vortices (see Fig. 1).

Liu's model is modified here in the following way: the strengths of the two vortices are not constant, but their ratio is to model the secondary vortex decay. So the angular velocity is not constant.

The values of Liu's parameter are

$$r'_i = b_0/2$$

$$\Gamma'_i = -0.3 \text{ to } -0.7\Gamma_i$$

$$h_0 = 0.577 b_o$$

The secondary vortex is introduced when the associated primary vortex reaches the altitude h_0.

Crosswind and Shear

Tombach[7] and Bilanin et al.[12] have shown that the vortex of opposite circulation to the shear decays more quickly. This vortex could even disappear and then the very hazardous phenomenon of solitary vortex could occur. In this case, the main mechanism of decay is not the linking instability.

The advection of the crosswind is taken into account by adding a term in Eq. (4):

$$\frac{dx_i}{dt} = w(z_i) + \sum_{j \neq i} \frac{\Gamma_j}{2\pi} \frac{y_j - y_i}{r_{ij}^2} + \frac{\Gamma'_i \cos\theta_i}{2\pi r'_i} \tag{8}$$

For the effect on vortex decay, we use a simple model proposed by Cox et al.[13] This model assumes that the decay of the vortex with the opposite sign vorticity from the crosswind is accelerated by applying a couple in the opposite sense to the vortex circulation:

$$\frac{d\Gamma}{dt} = -\frac{2}{3} C_{DV} \sigma w_0 b_0$$

where C_{DV} is the viscous coefficient caused by crosswind. Bilanin et al.[12] showed that the decay rate of the vortex with the same sign vorticity as the crosswind is not influenced significantly. Therefore, that vortex is not modified in VORTEX.

Linking Instability—Bursting—Core Radius

These three phenomena are taken into account with simple empirical models. The linking time T_c (Ref. 14), time taken for the Crow instability to grow sufficiently for the vortices to touch, can be expressed in terms of rms turbulence velocity:

$$T_c = 0.82\Lambda^{1/3}/qb_0^{1/3}$$

The bursting time T_b (Ref. 15) is

$$T_b = 0.39(b_0/\varepsilon)^{1/3}$$

In practice, for core radius growth,[16] we use

$$r_c = \max(r_{c0}, 0.0125\sqrt{\Gamma_0 t})$$

Validation

The validation of VORTEX was done using a Navier–Stokes solver available at CERFACS (NTMIX). The numerical scheme is given in Lele[17] and Poinsot and Lele.[18] Here we illustrate only its main features. NTMIX solves the fully compressible two-dimensional Navier–Stokes equations. For the spatial differentiation, high-order compact schemes of spectral-like resolution are used and for time integration, a third-order Runge–Kutta method.

Initialization

We use Lamb's vortex whose stream function is

$$\psi = -g\,\ell n(r^2 + r_c^2)$$

where g is related to the circulation of the vortex. The Reynolds number of the computation is

$$Re = \frac{u_{\theta_{max}} r_c}{\nu} = \frac{g}{\nu} = \frac{\Gamma}{4\pi\nu} = \frac{1}{4\pi} Re_\Gamma$$

The initialization is made with four vortices: two real vortices and their mirror images to ensure the inviscid slip condition at the wall (the no-slip condition is verified by imposing a zero parallel velocity at the wall). The computational domain is presented in Fig. 1. The secondary vortices appearing in this figure are created during the computation and are not initialized.

Rebound

In a first approach the ground effect was studied with laminar flows. The boundary conditions are vertical plane of symmetry ($x = 0$), no-slip wall at bottom, and no reflecting for the two other sides. Two vortices (real and mirror image) are initially put at $x^* = x/b = 0.4$ and $y^* = y/b = \pm 1.0$. The initial core radius is set to $r_{c0}^* = r_{c0}/b = 0.1$. Figure 2 shows the evolution of the vorticity field for three different time steps obtained at Re equal to 600 on a 121 × 257 grid. The simulation lasts up to a dimensionless time $t^* = u_\theta t/b_0$ of 15. As explained by Harvey and Perry,[10] the primary vortex induces a very strong vorticity sheet because of the adverse pressure gradient during its descent. This vorticity sheet becomes unstable and detaches from the wall creating a secondary vortex.

Figure 2 shows the contours of normalized vorticity ω^* from -5.0 to 5.0 with $\Delta\omega^* = 0.5$.

A phenomenon not obvious in the figures is the creation of a tertiary vortex (see Fig. 2b) because of a weak and thin vortex sheet induced by the secondary vortex. This tertiary vortex disappears quickly. The secondary vortex makes the primary one rise up and it rolls over it. In moving away from the wall they elongate the vorticity sheet at the wall until it breaks. Orlandi[19] reports similar results by solving the Navier–Stokes equations in the vorticity–stream function formulation. His computations are made with Re equal to 8.0 ×

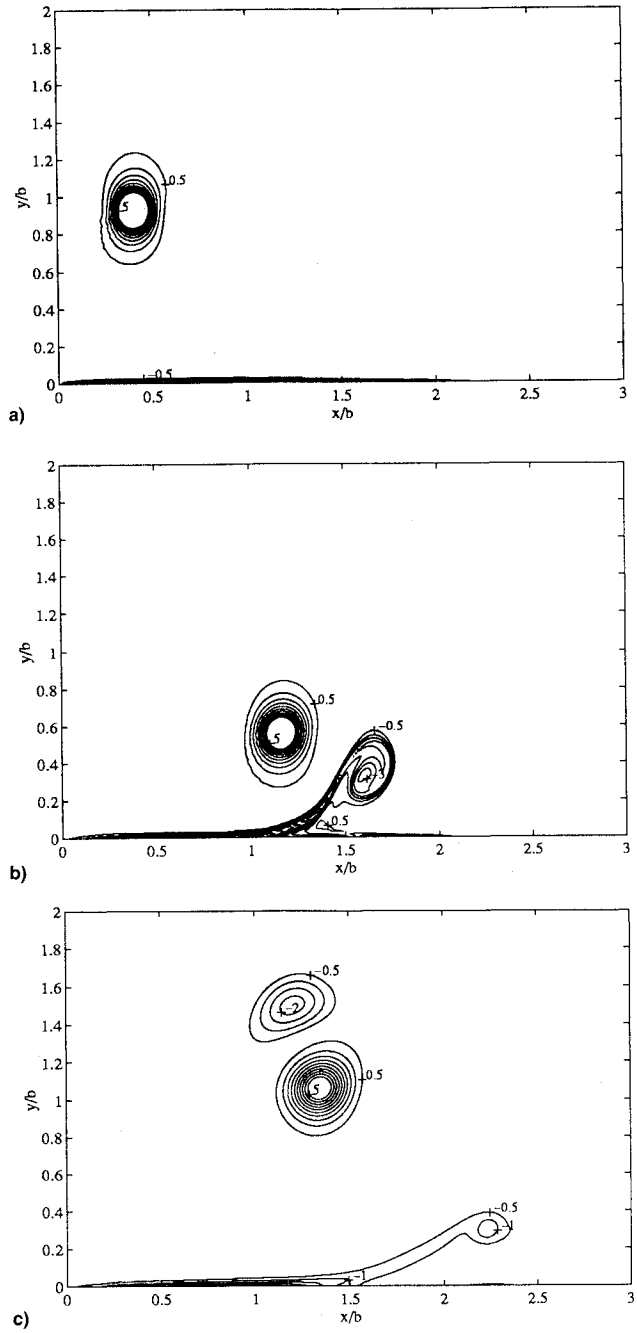

Fig. 2 Contours of vorticity (NTMIX). t^* = a) 0, b) 8, and c) 15.

10^2 and a different initialization of the vortex dipole. He computes a ratio between the circulations of the primary and secondary vortices of $\Gamma_r = |\Gamma'/\Gamma|$ equal to 0.476. For the case presented in Fig. 2, we compute the ratio Γ_r using three methods. The results are summarized in Table 1. These three methods assume that the vorticity distribution follows the ideal Lamb's vorticity distribution.

The values of g the circulation parameter used in DNS computation and r_c are computed using these three methods. The first method uses the fact that at r_c the vorticity is one-quarter of the maximal vorticity (noted $\omega_{max}/4$). The two others use the same nonlinear regression method on a complete or reduced set of data. The scatter of the results is relatively important, but the trends are the same. There is also scatter for the computed ratio Γ_r (see Table 1), but the results at $t^* = 9$ are in good agreement with those of Orlandi.[19] We find $0.386 < \Gamma_r < 0.450$.

The variation of the total circulation as a function of time is given in Fig. 3. These results may be compared with the results obtained by Zheng and Ash.[20] Their laminar computations were made with a circulation based Reynolds number Re_Γ equal to 7500.

Crosswind Simulations

Presentation

As for the other meteorological parameters, a new similarity number to represent the effects of crosswind and shear is defined:

$$W_S = w_0 b_0 / \Gamma_0$$

This number represents the ratio between the crosswind velocity w_0 and the velocity induced by the vortices. In the limits of the VORTEX code, W_S only controls the vortex trajectory. The vortex radius should play no role. The NTMIX computations are made in a domain $(-3 < x^* < 3,\ 0 < y^* < 2)$ on a 363×121 grid. The boundary conditions are a subsonic inlet condition with an imposed linear wind profile (see Fig. 1), no slip wall at bottom, and no reflecting for the two other sides. There is no symmetry plane.

Effects of Core Radius

Three computations were made with the same initial strength of the vortices ($g_0^* = g_0/bc = 0.3$) and Re equal to 600. The initial core radius r_{c0}^* are, respectively, 0.15, 0.1, 0.05. The trajectories of the two primary vortices (position of maximum vorticity as a function of time) are shown in Fig. 4. The three trajectories are quite similar. This clearly shows that the main effect of the crosswind is the advection of the vortices in agreement with the inviscid theory. This figure shows another important fact: the altitude of rebound h_0 depends on the core radius. The rebound occurs at higher altitude when the core is larger.

Effects of Vortex Strength

Like for the core radius, three computations were performed to study the effect of vortex strength (or Reynolds number) on the trajectory of the vortices. The three strengths are g^* equal to 0.02, 0.03, and 0.04 with the same core radius r_{c0}^* equal to 0.1.

Table 1 Computed ratios

t^*	$\omega_{max}/4$	Complete regression	Reduced regression
9	0.401	0.386	0.450
17	0.581	0.530	0.607

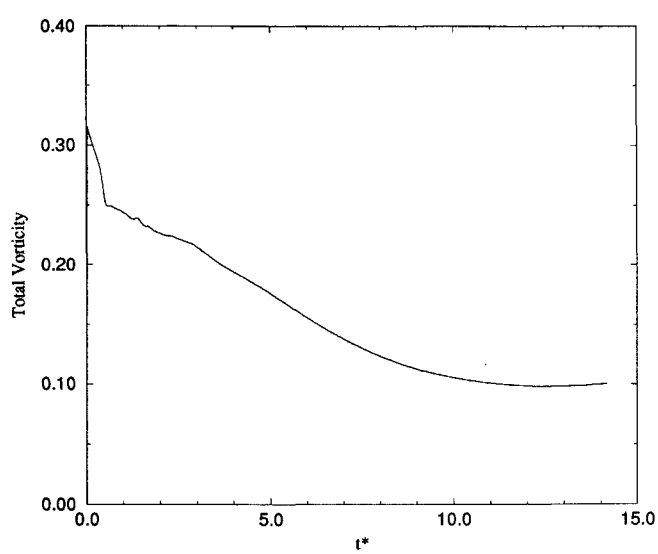

Fig. 3 Variation of total circulation.

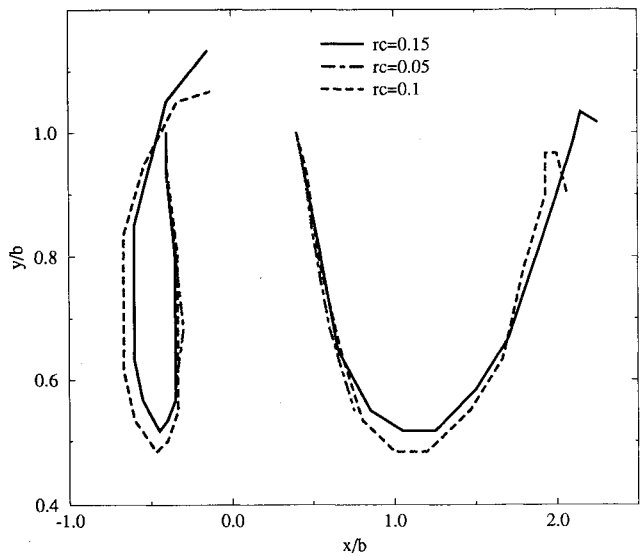

Fig. 4 Effect of core size (trajectories).

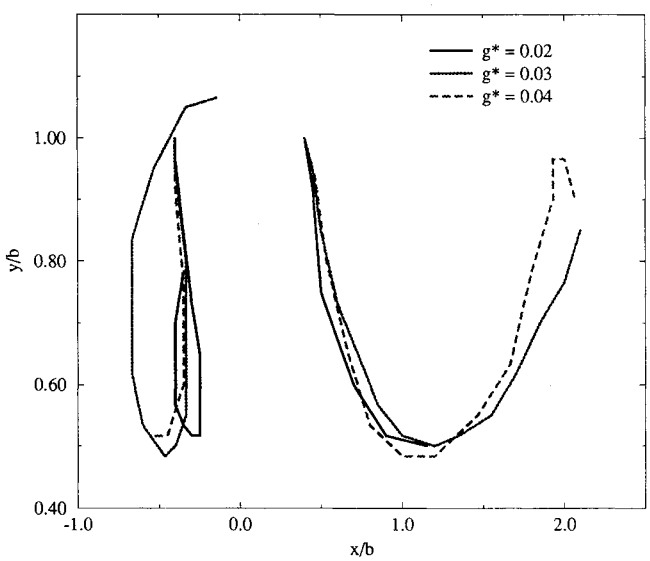

Fig. 5 Effect of vortex strength (trajectories).

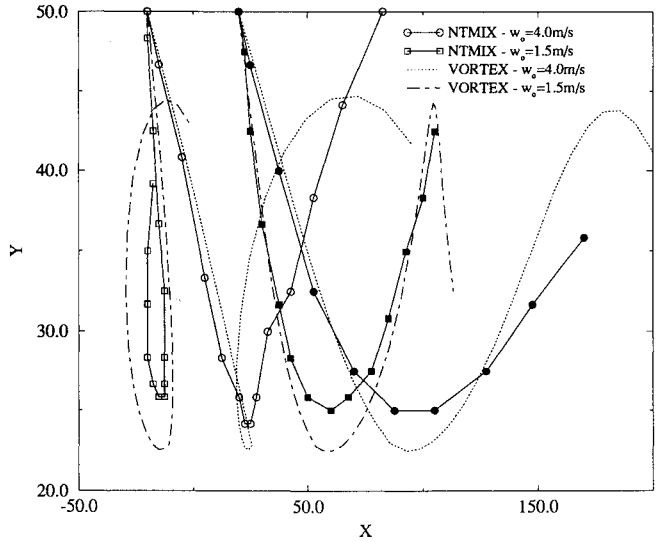

Fig. 6 First comparison VORTEX–NTMIX (trajectories).

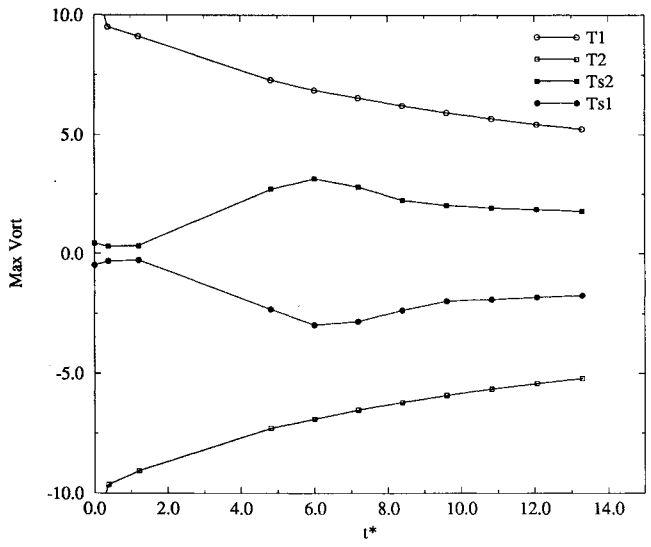

Fig. 7 Maxima of vorticity vs time.

The trajectory varies with the initial circulation of rebound (see Fig. 5). As shown by Orlandi,[19] the effect of the secondary vortex is more important when the strength of the primary vortex increases.

Comparison VORTEX–NTMIX

To obtain a first validation of the rebound model with crosswind, two computations were made with VORTEX and NTMIX. The conditions are the following: initial circulation 300 m^2/s, initial spacing 40 m, crosswind 1.5 m/s (case 1), and 4.0 m/s (case 2). These parameters lead to W_S numbers 0.2 (case 1) and 0.533 (case 2). Furthermore, in VORTEX the parameter C_D is set to 0.2 and we assume that there is neither turbulence nor stratification. The ratio between the primary and secondary vortices strengths is 0.45 and the altitude of rebound equal to $0.577b_0$. For NTMIX, the boundary conditions are the same as for the crosswind simulations and the initial conditions are computed so that W_S matches the real one. In Fig. 6 the results obtained with NTMIX and VORTEX are compared. A satisfactory agreement is obtained in most cases.

The first remark is that case 1 is the most hazardous from an operational point of view. The upwind vortex rebounds and stays near the runway axis. For case 2, the two vortices are swept from the runway and a following aircraft can land safely.

These results are in agreement with the experiments. If we consider now the hypotheses of the rebound model, we can notice that the assumption of constant altitude of rebound is not verified. This altitude is between $0.6-0.646b_0$. The other parameters for the rebound model are the constant spacing between the primary and the secondary vortices and the ratio between their circulation.

To assess these hypotheses, the maxima of vorticity as a function of time for primary vortices (T1, left unfilled circle and T2, right unfilled square) and secondary vortices (Ts1, left filled circle and Ts2, right filled square), are presented in Fig. 7 and the trajectories of these points in Fig. 8. The ratio of the maximum of absolute vorticity of each vortex varies from 0.317 up to 0.432, and the distance between them from 0.458 to 0.568. If the average parameters obtained with NTMIX are used in VORTEX, a better agreement between the two computations is obtained.

These first results are encouraging and prove that our approach is meaningful. We have now to improve the rebound model to take into account the variations of altitude of rebound and strength ratio with Reynolds number and core size.

Comparison VORTEX–Experimental Data

The experimental data of Idaho Falls,[21] distributed by the FAA, are also used to validate the VORTEX code. The test

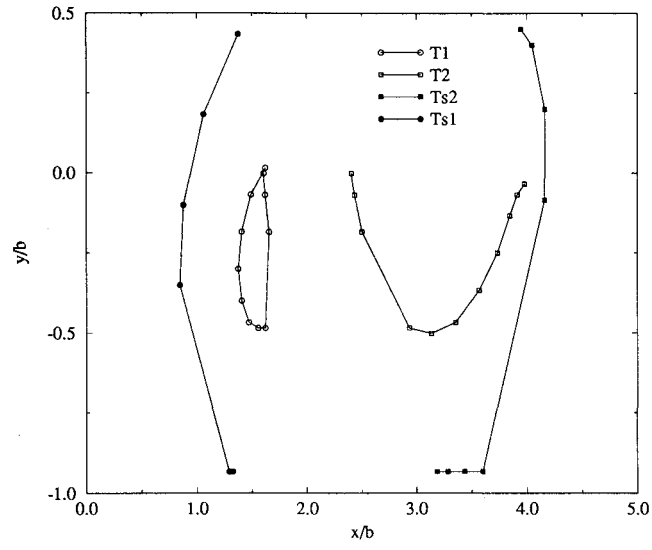

Fig. 8 Trajectories of primary and secondary vortices.

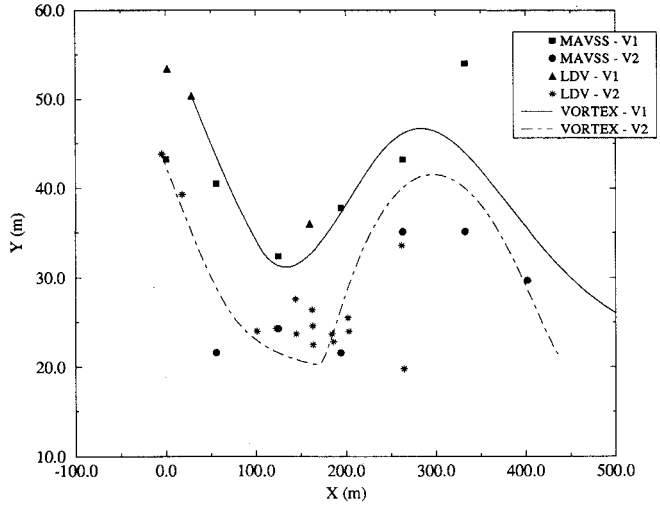

Fig. 9 Comparison VORTEX–experiment (trajectories).

case chosen is run 9 of a Boeing 757. The data of the experiment are used as initial data in VORTEX. There is a fair agreement between the results presented in Fig. 9. The experimental data are obtained either with a laser Doppler velocimeter (LDV) or a mono acoustic vortex sensing system (MAVSS). The altitude of rebound used in VORTEX is set with the experimental data [$h_0(V1) = 0.9b_0$ and $h_0(V2) = 0.577b_0$]. The meteorological parameters ($q = 0.161$, $N = 0.025$, wind profile) are set using the data recorded during the run.[22] The decay obtained with VORTEX differs from the experimental result.

This comparison confirms that VORTEX is able to model the behavior of vortices near the ground, but the modeling of the altitude of rebound, turbulence, and stratification are to be improved.

Conclusions

A tool was developed to define, from an operational point of view, the safe separation between aircraft at landing and takeoff.

We have described here how the model predicting vortex evolution after being shed from the airplane is developed and validated. The developed model takes into account all of the parameters influencing the decay and transport of the vortices: interaction with the ground, crosswind, stratification, etc.

The first results show that the general behavior of the vortices is well represented. But as usual with simple models, the model requires a great amount of validation. To validate not only the results, but also the hypotheses advanced computations with NTMIX, a DNS code was made. The first results are encouraging and we will, in the near future, make large eddy simulations to reach more realistic Reynolds numbers of the flowfield.

The results obtained with Greene's model[4] seem to be in good agreement with the experiments for the viscous and turbulence effects[23] and stratification,[24] but we will investigate further the effect of atmospheric turbulence to improve the modeling of turbulence in VORTEX (Ref. 25). The main effect of the crosswind on the vortices when they are out of ground effect is the advection. The induced viscous decay is less important at the beginning of the process in laminar flows. For the rebound, the numerical simulations are in agreement with the experimental work, which explains the rebound by the creation of a secondary vortex. We show that even a tertiary vortex is created, but that it decays very quickly and has no effect on the trajectory of the primary one. We show also that our model is not sufficient to simulate this viscous phenomenon because the altitude of rebound is related to the vortex core radius and the Reynolds number. This has to be investigated further with also the effect of vertical wind shear.[26]

Acknowledgments

This work was supported by the Service Technique Navigation Aérienne under Research Grant STNA/S4/93/47. The authors would like to thank C. Le Roux for helpful discussions, M. Baum for NTMIX developments, and LATEX help.

References

[1]Krasny, R., "A Study of Singularity Formation in a Vortex Sheet by the Point-Vortex Approximation," *Journal of Fluid Mechanics*, Vol. 167, 1986, pp. 65–93.

[2]Krasny, R., "Computation of Vortex Roll-Up in the Trefftz Plane," *Journal of Fluid Mechanics*, Vol. 184, 1987, pp. 123–155.

[3]Escande, B., "Analyse Paramétrique du Comportement Avion dans une Turbulence de Sillage: Modélisation et Développement du Logiciel de Simulation," ONERA, RT 19/5158 SY, March 1993.

[4]Greene, G., "An Approximate Model of Vortex Decay in the Atmosphere," *Journal of Aircraft*, Vol. 23, No. 7, 1986, pp. 566–573.

[5]Donaldson, C. D., and Bilanin, A., "Vortex Wakes of Conventional Aircraft," *AGARDograph*, May 1975.

[6]Lamb, H., *Hydrodynamics*, Dover, New York, 1932.

[7]Tombach, I., "Observations of Atmospheric Effects on Vortex Wake Behavior," *Journal of Aircraft*, Vol. 10, No. 11, 1973, pp. 641–647.

[8]Saffman, P., "The Approach of a Vortex Pair to a Plane Surface in Inviscid Fluid," *Journal of Fluid Mechanics*, Vol. 92, 1979, pp. 497–503.

[9]Dee, F., and Nicholas, O., "Flight Measurements of Wing Tip Vortex Motion Near the Ground," Royal Aircraft Establishment TR 68007, 1968.

[10]Harvey, J., and Perry, F., "Flowfield Produced by Trailing VorNtices in the Vicinity of the Ground," *AIAA Journal*, Vol. 9, No. 8, 1971, pp. 1659, 1660.

[11]Liu, H., "Tow-Tank Simulation of Vortex Wake Dynamics," *FAA Proceedings of the Aircraft Wake Vortices Conference*, FAA, Washington, DC, 1991, pp. 32-1, 32-26.

[12]Bilanin, A., Teske, M., and Hirsh, J., "Neutral Atmospheric Effects on the Dissipation of Aircraft Vortex Wakes," *AIAA Journal*, Vol. 16, No. 9, 1978, pp. 956–961.

[13]Cox, C., Fairbanks, M., and McCulloch, R., "Functional Design Specification of a Model of Aircraft Wake Vortices," SMITH, TR-92/232/1.0, London, 1992.

[14]Crow, S., "Stability Theory for a Pair of Trailing Vortices," *AIAA Journal*, Vol. 8, No. 12, 1970, pp. 2172–2179.

[15]Tombach, I., Lissaman, P., and Mullen, J., "Aircraft Wake Vortex Behaviour and Decay near the Ground," *Proceedings of the Aircraft Wake Vortices Conference*, FAA-RD-77-68, Washington, DC, 1977, pp. 31–46.

[16]Iversen, J., "Correlation of Turbulent Trailing Vortex Decay Data," *Journal of Aircraft*, Vol. 13, No. 5, 1976, pp. 338–342.

[17]Lele, S. K., "Compact Finite Difference Schemes with Spectral-Like Resolution," *Journal of Computational Physics*, No. 103, 1992, pp. 16–42.
[18]Poinsot, T., and Lele, S., "Boundary Conditions for Direct Simulations of Compressible Viscous Flows," *Journal of Computational Physics*, Vol. 101, July 1992, pp. 104–129.
[19]Orlandi, P., "Rebound of Vortex Dipole," *Physics of Fluids A*, Vol. 2, No. 8, 1990, pp. 1429–1436.
[20]Zheng, Z., and Ash, R., "Viscous Effects on a Vortex Wake in Ground Effect," *FAA Proceedings of the Aircraft Wake Vortices Conference*, FAA, Washington, DC, 1991.
[21]Garodz, L. J., and Clawson, K. L., "Vortex Wake Characteristics of B757-200 and B767-200 Aircraft Using the Tower Fly-By Technique," Environmental Research Lab., Air Resources Lab., TM-199, Vols. 1 and 2, National Oceanographic and Atmospheric Administration, Jan. 1993.
[22]Janota, P., "Atmospheric and Vortex Description for Idaho Falls B-757 Run 9 on September 25, 1990," System Resources Corp., Lexington, MA, April 1994.
[23]Köpp, F., "Doppler Lidar Investigation of Wake Vortex Transport Between Closely Spaced Parallel Runways," *AIAA Journal*, Vol. 32, No. 4, 1994, pp. 805–810.
[24]Sarpkaya, T., "Trailing Vortices in Homogeneous and Density-Stratified Media," *Journal of Fluid Mechanics*, Vol. 136, 1983, pp. 85–109.
[25]Risso, F., Corjon, A., and Stoessel, A., "Direct Numerical Simulation of Trailing Vortices in Homogeneous Turbulence," AIAA Paper 96-0802, Jan. 1996.
[26]Corjon, A., and Poinsot, T., "Wake Vortices Behavior Near the Ground," *Proceedings of 2nd International Workshop on Vortex Flows and Related Numerical Methods*, CUSLN, Edmonton, Canada, 1995.